Supplementary Information to Time–scale dependent relations between Earth Observation based proxies of vegetation productivity

Nora Linscheid[1,2], Miguel D. Mahecha[3,4], Anja Rammig[2], Nuno Carvalhais[1,5], Fabian Gans[1], Jacob A. Nelson[1], Sophia Walther[1], Ulrich Weber[1], Markus Reichstein[1,6,7]

[1]Max Planck Institute for Biogeochemistry, Hans–Knoell–Str. 10, 07745 Jena, Germany
[2]TUM School of Life Sciences Weihenstephan, Technical University of Munich, Hans–Carl–von–Carlowitz–Platz 2, 85354 Freising, Germany
[3]Remote Sensing Center for Earth System Research, Leipzig University, Talstr. 35, 04103 Leipzig, Germany
[4]Helmholtz Centre for Environmental Research UFZ, Permoserstr. 15, 04318 Leipzig, Germany
[5]Departamento de Ciencias e Engenharia do Ambiente, DCEA, Faculdade de Ciencias e Tecnologia, FCT Universidade Nova de Lisboa, Caparica, Portugal
[6]Michael Stifel Center Jena for Data–Driven & Simulation Science, Ernst–Abbe–Platz 2, 07743 Jena, Germany
[7] German Centre for Integrative Biodiversity Research (iDiv), Deutscher Platz 5e, 04103 Leipzig, Germany.

Corresponding author: Nora Linscheid, nlinsch@bgc-jena.mpg.de

Supplementary Figures

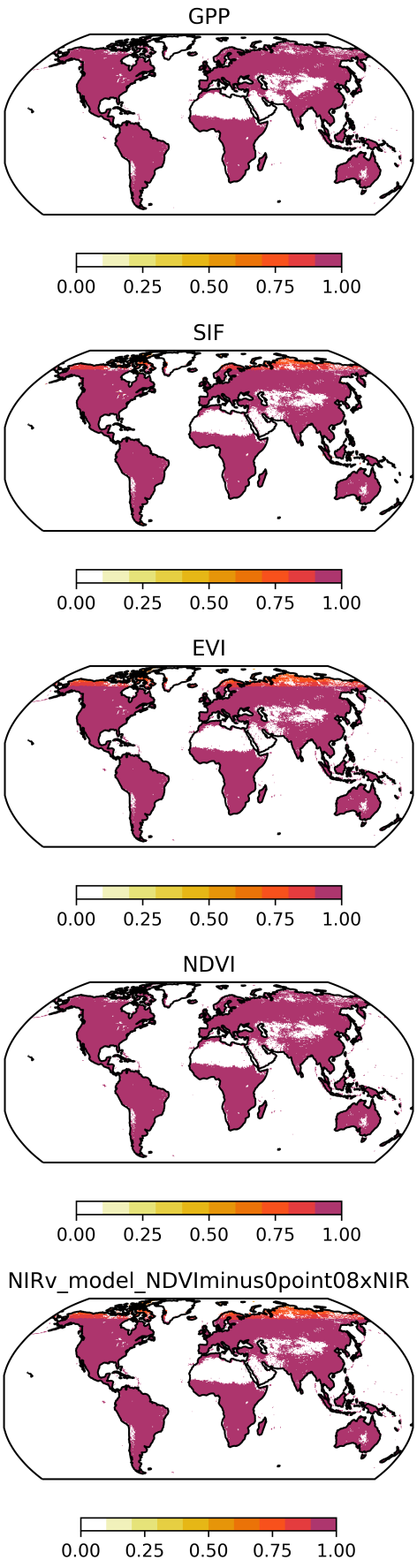

Figure S1: Fraction of non–missing values per grid cell prior to gapfilling.

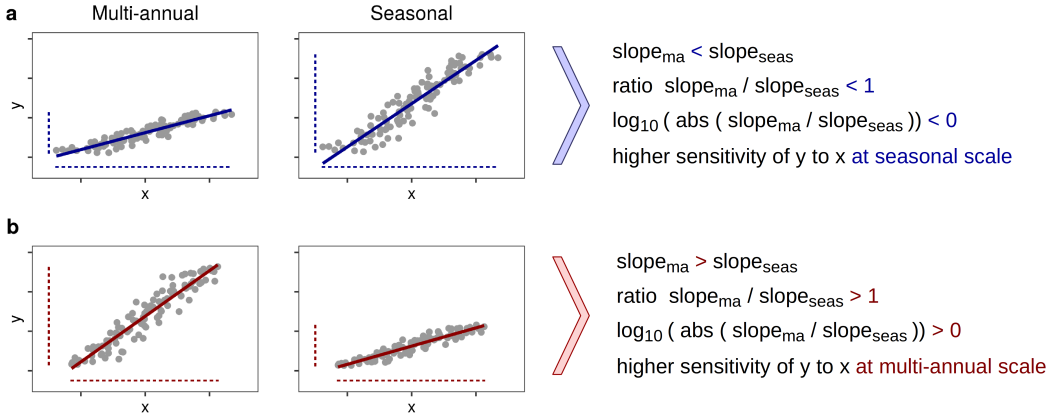

Figure S2: Schematic representation of slope ratio calculation and interpretation. Theoretical examples of a time series where **a.** the multi–annual slope is lower than the seasonal slope, and **b.** the multi–annual slope is higher than the seasonal slope. Points denote data, solid lines denote linear regression lines, and dotted lines illustrate the data variance along each axis. The more strongly y varies with x, the higher the slope and the more "sensitive" y is to changes in x. In panel **a**, y varies more strongly with x at seasonal than multi–annual scale, thus the seasonal slope is higher. This is reflected in a log10(abs($slope_{ma}$/$slope_{seas}$)) ratio below zero. Panel **b** illustrates the reverse. Color code is based on the color scale in the remaining figures of this paper where logarithmic ratios below zero (higher seasonal slopes) are shown in blue, and logarithmic ratios above zero (higher multi–annual slopes) are shown in red.

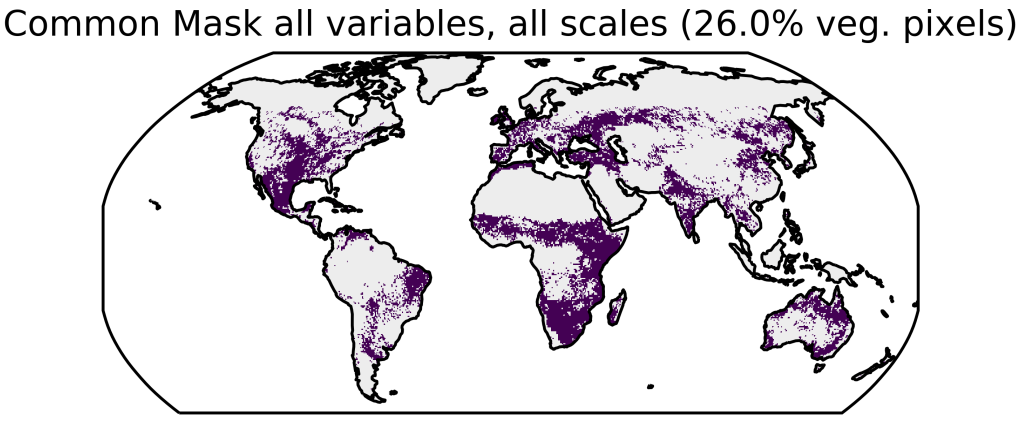

Figure S3: Land cover pixels used for all analyses comparing across variable pairs. After filtering for sufficient signal amplitude, significance of correlation, and discarding outlier values, 27% of vegetated land pixels remained.

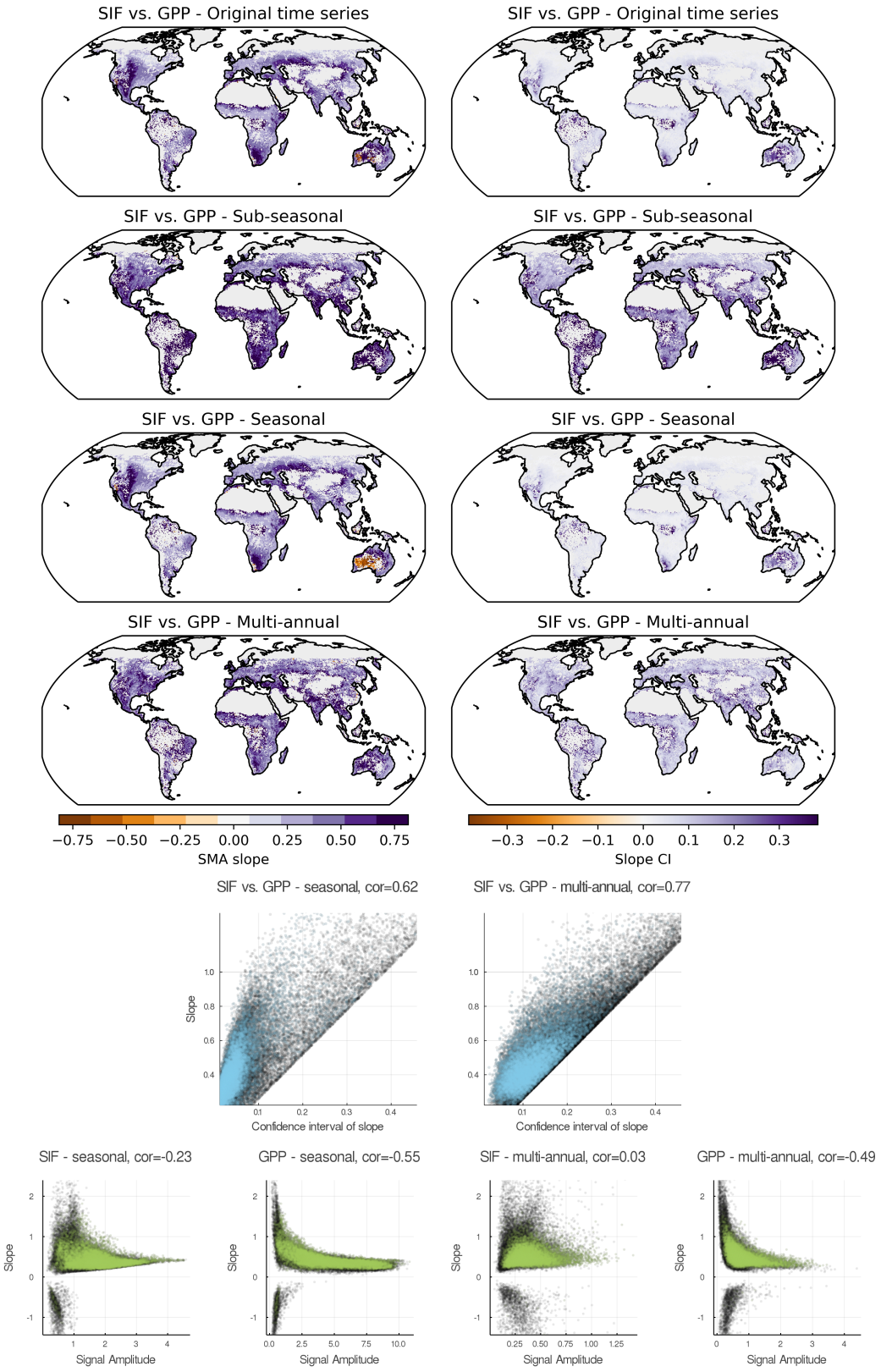

Figure S4: Time–scale specific slopes between SIF vs. GPP. Top: Map of pixel–wise slopes (left) and confidence intervals of slopes (right). Middle: Slopes are plotted against their confidence intervals for seasonal (left) and multi–annual scales (right). Bottom: Scale–specific slopes are compared against matching scale–specific signal amplitudes separately for seasonal (left) and multi–annual time scale (right). Blue/Green points are retained in the analysis, grey points are filtered out. Correlations were calculated as Pearson correlation between non–filtered points. Slope units are [mW m^{-2} sr^{-1} nm^{-1} / gC m^{-2} d^{-1}]; *gC: gram Carbon*

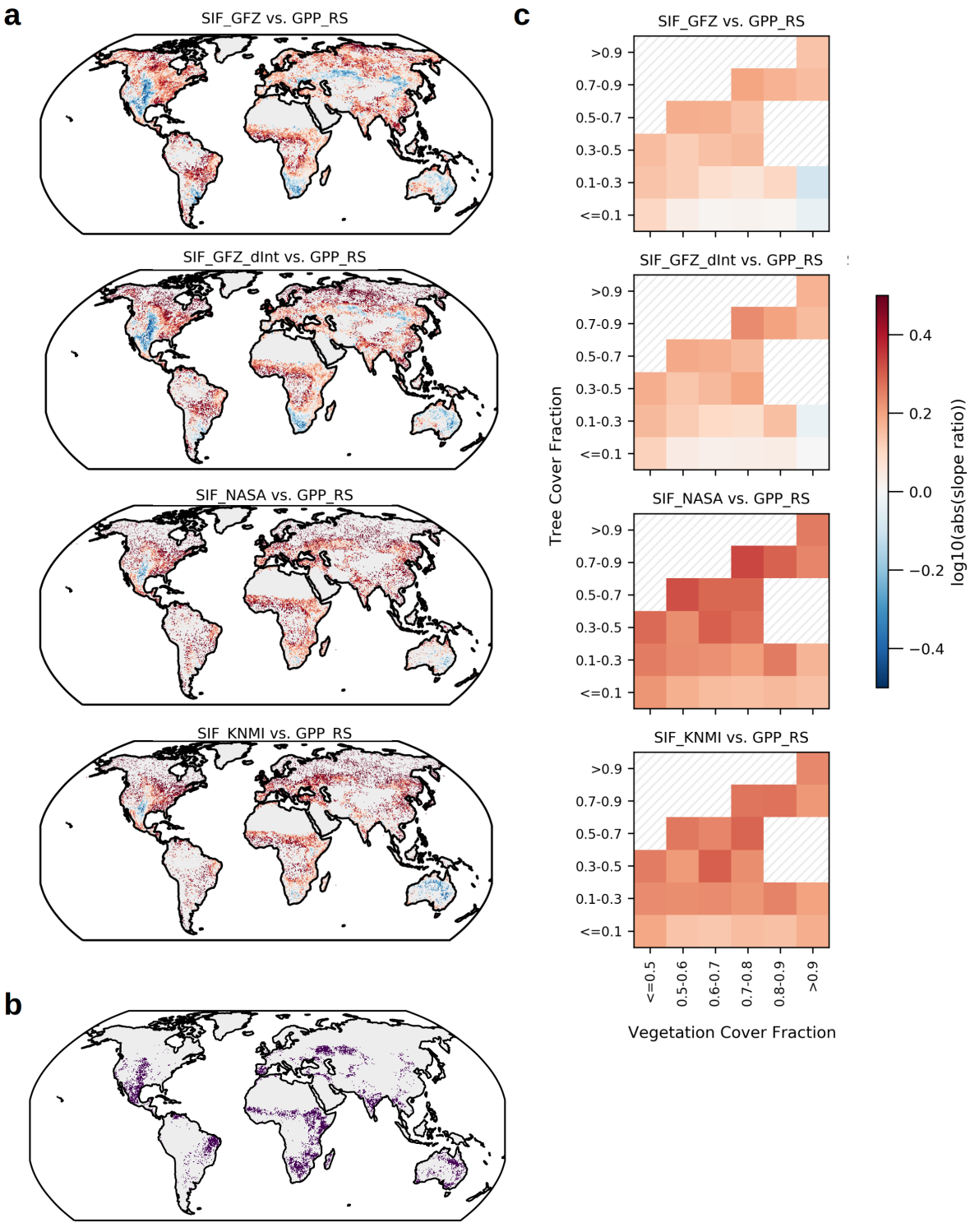

Figure S5: Slope ratios between GPP_{FC} (here: GPP_RS) and a SIF ensemble. **a.**Slope ratios for different GOME–2 SIF datasets from GFZ (SIF_GFZ, initial dataset), a daily integral calculated from SIF_GFZ (SIF_GFZ_dInt) NASA (SIF_NASA) and KNMI (SIF_KNMI), **b.** map of pixels passing all filtering criteria for all datasets included in this comparison, i. e. 4818 pixels, or 8.8% of vegetated land pixels, **c.** Heatmaps of mean slope ratios along gradients of tree cover and vegetation cover for each variable combination, based on common pixels displayed in b.

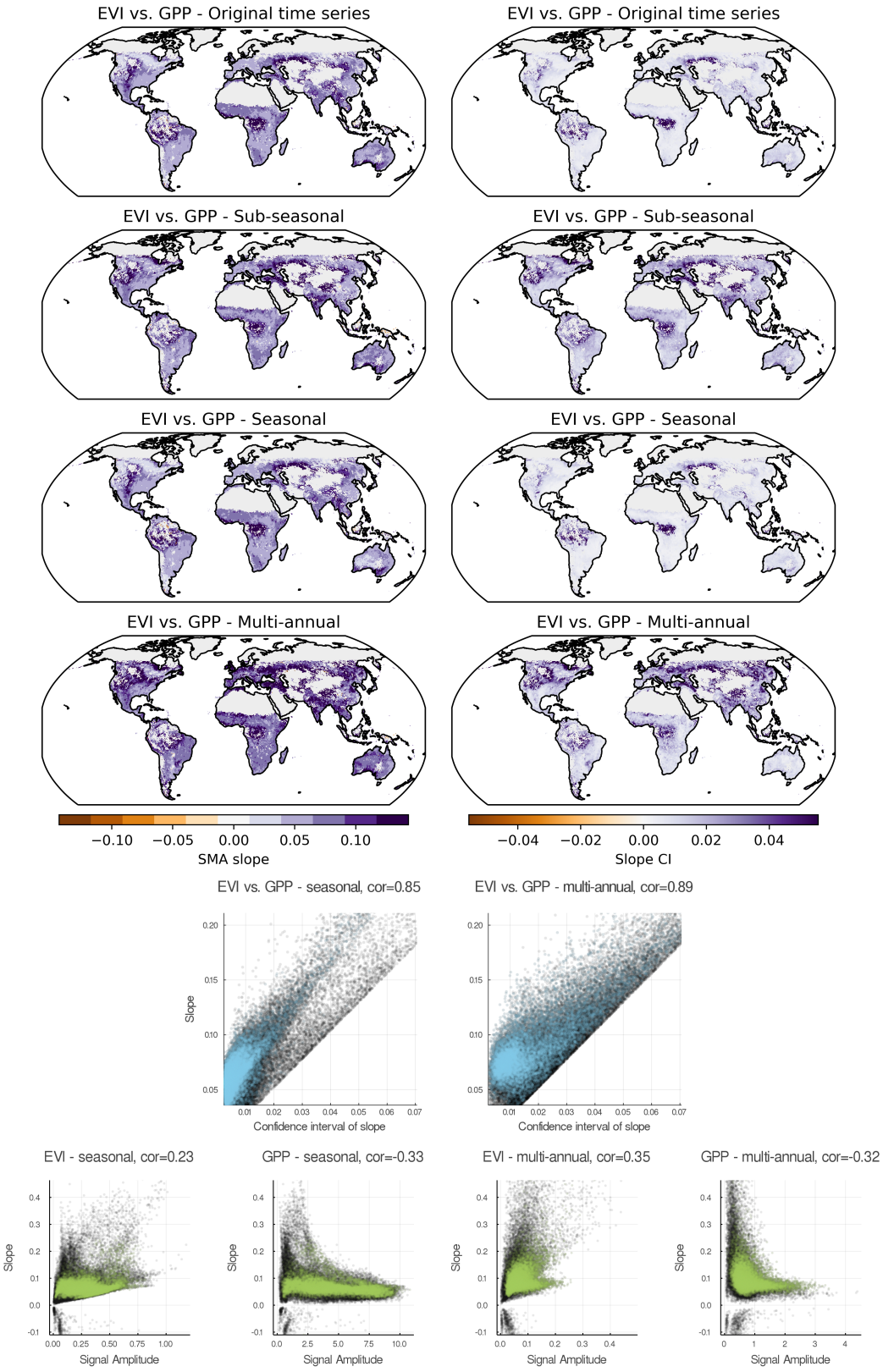

Figure S6: Time–scale specific slopes between EVI vs. GPP. Top: Map of pixel–wise slopes (left) and confidence intervals of slopes (right). Middle: Slopes are plotted against their confidence intervals for seasonal (left) and multi–annual scales (right). Bottom: Scale–specific slopes are compared against matching scale–specific signal amplitudes separately for seasonal (left) and multi–annual time scale (right). Blue/Green points are retained in the analysis, grey points are filtered out. Correlations were calculated as Pearson correlation between non–filtered points.

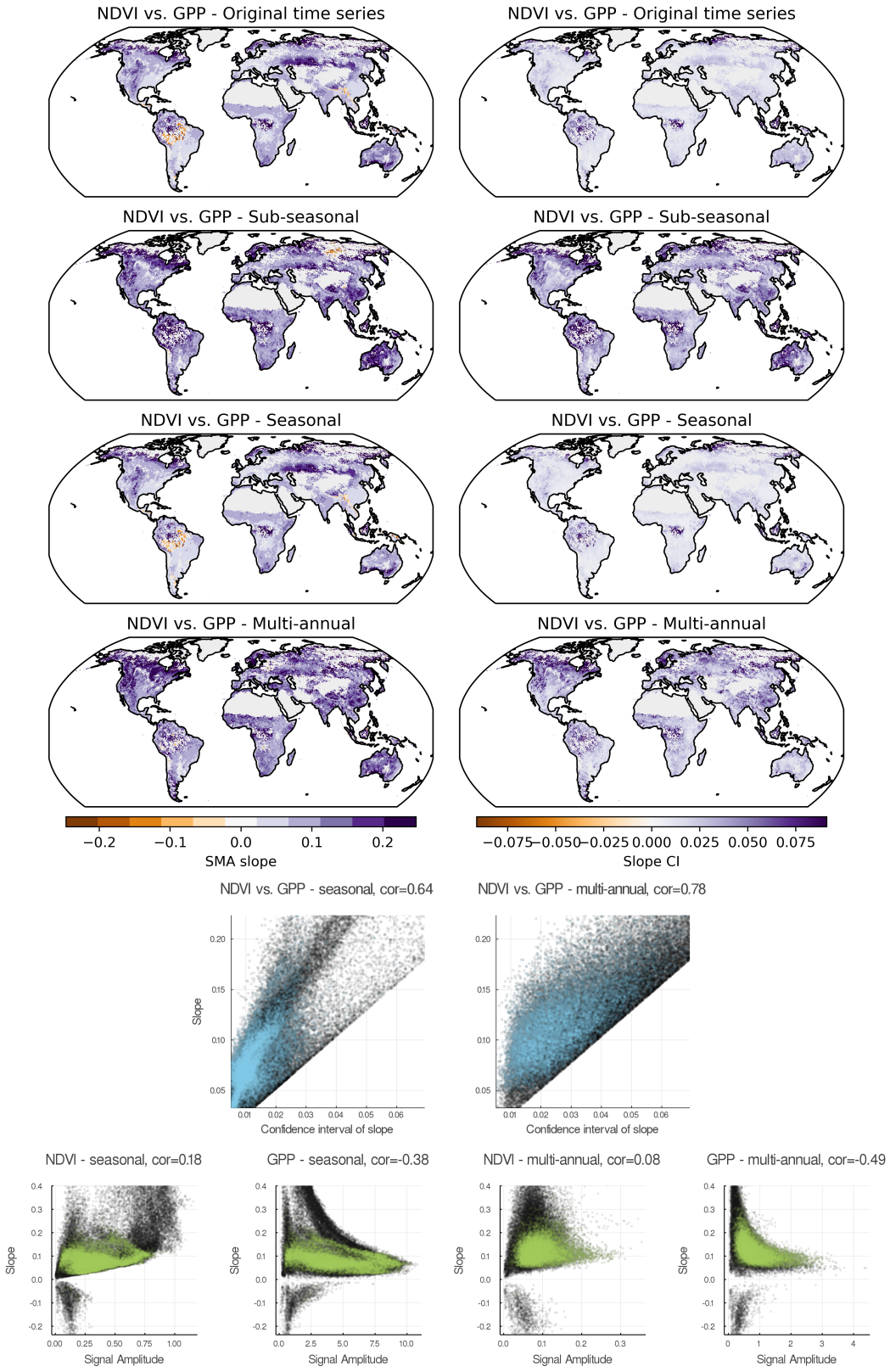

Figure S7: Time–scale specific slopes between NDVI vs. GPP. Top: Map of pixel–wise slopes (left) and confidence intervals of slopes (right). Middle: Slopes are plotted against their confidence intervals for seasonal (left) and multi–annual scales (right). Bottom: Scale–specific slopes are compared against matching scale–specific signal amplitudes separately for seasonal (left) and multi–annual time scale (right). Blue/Green points are retained in the analysis, grey points are filtered out. Correlations were calculated as Pearson correlation between non–filtered points.

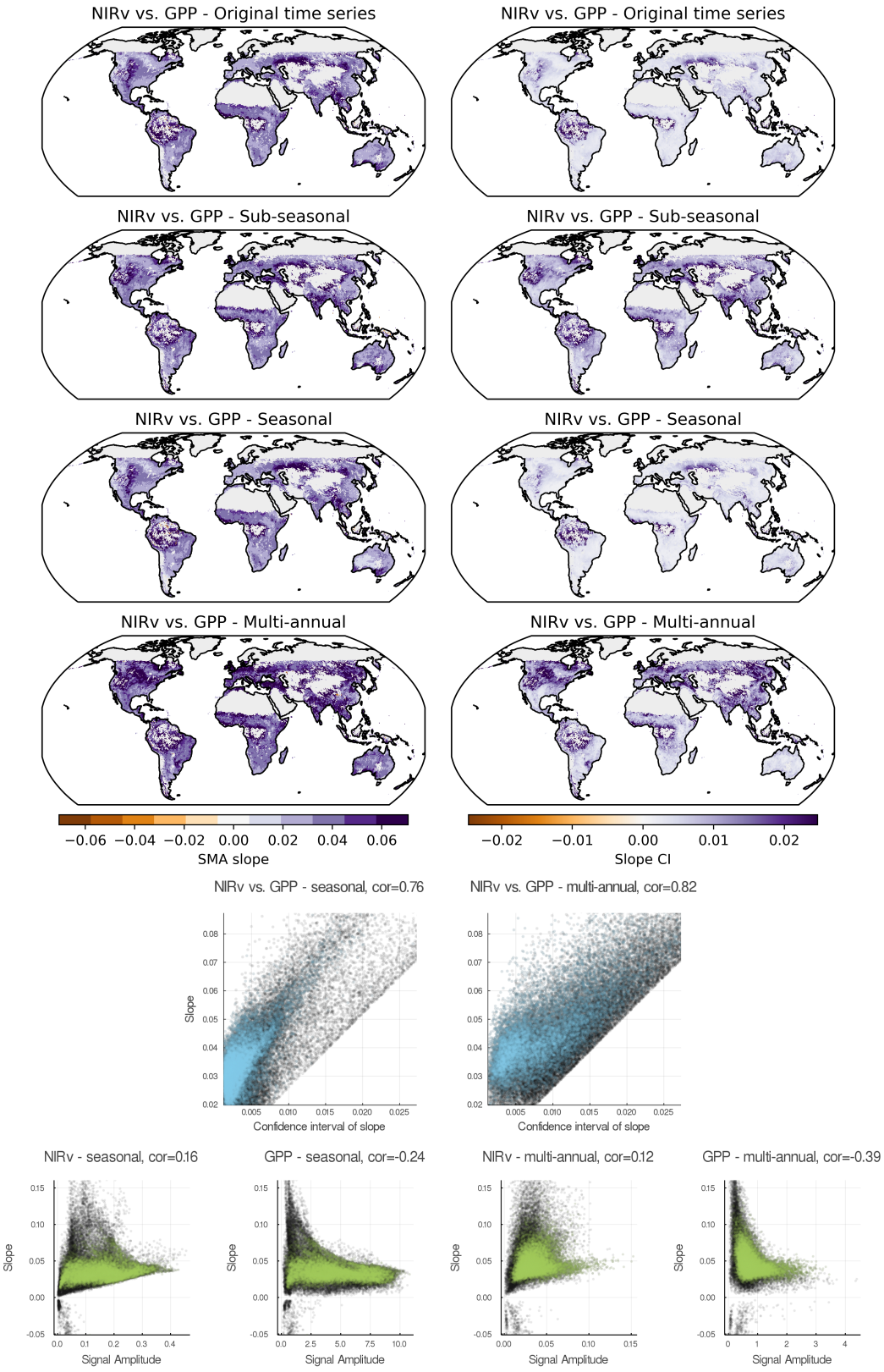

Figure S8: Time–scale specific slopes between NIRv vs. GPP. Top: Map of pixel–wise slopes (left) and confidence intervals of slopes (right). Middle: Slopes are plotted against their confidence intervals for seasonal (left) and multi–annual scales (right). Bottom: Scale–specific slopes are compared against matching scale–specific signal amplitudes separately for seasonal (left) and multi–annual time scale (right). Blue/Green points are retained in the analysis, grey points are filtered out. Correlations were calculated as Pearson correlation between non–filtered points.

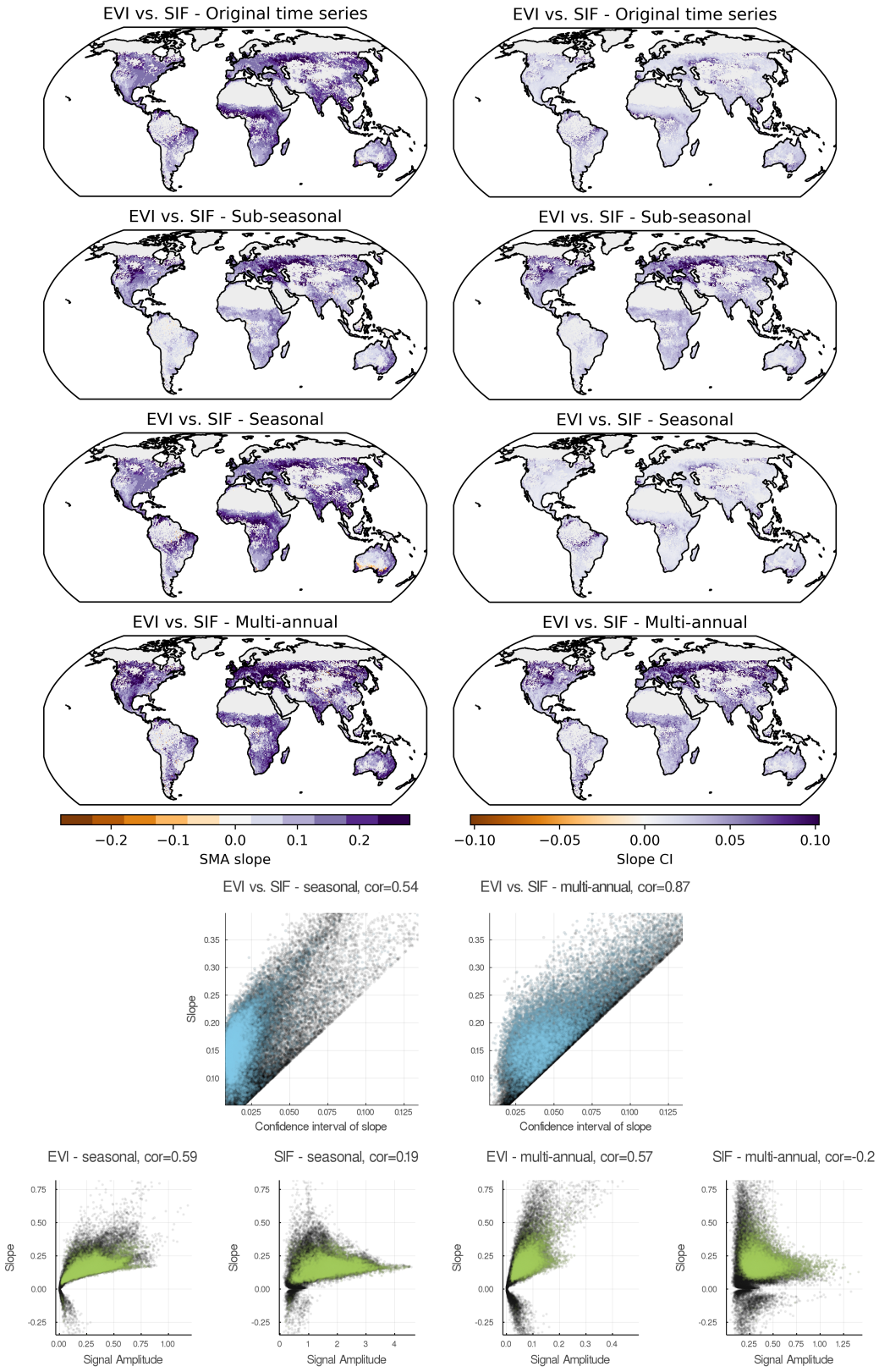

Figure S9: Time–scale specific slopes between EVI vs. SIF. Top: Map of pixel–wise slopes (left) and confidence intervals of slopes (right). Middle: Slopes are plotted against their confidence intervals for seasonal (left) and multi–annual scales (right). Bottom: Scale–specific slopes are compared against matching scale–specific signal amplitudes separately for seasonal (left) and multi–annual time scale (right). Blue/Green points are retained in the analysis, grey points are filtered out. Correlations were calculated as Pearson correlation between non–filtered points.

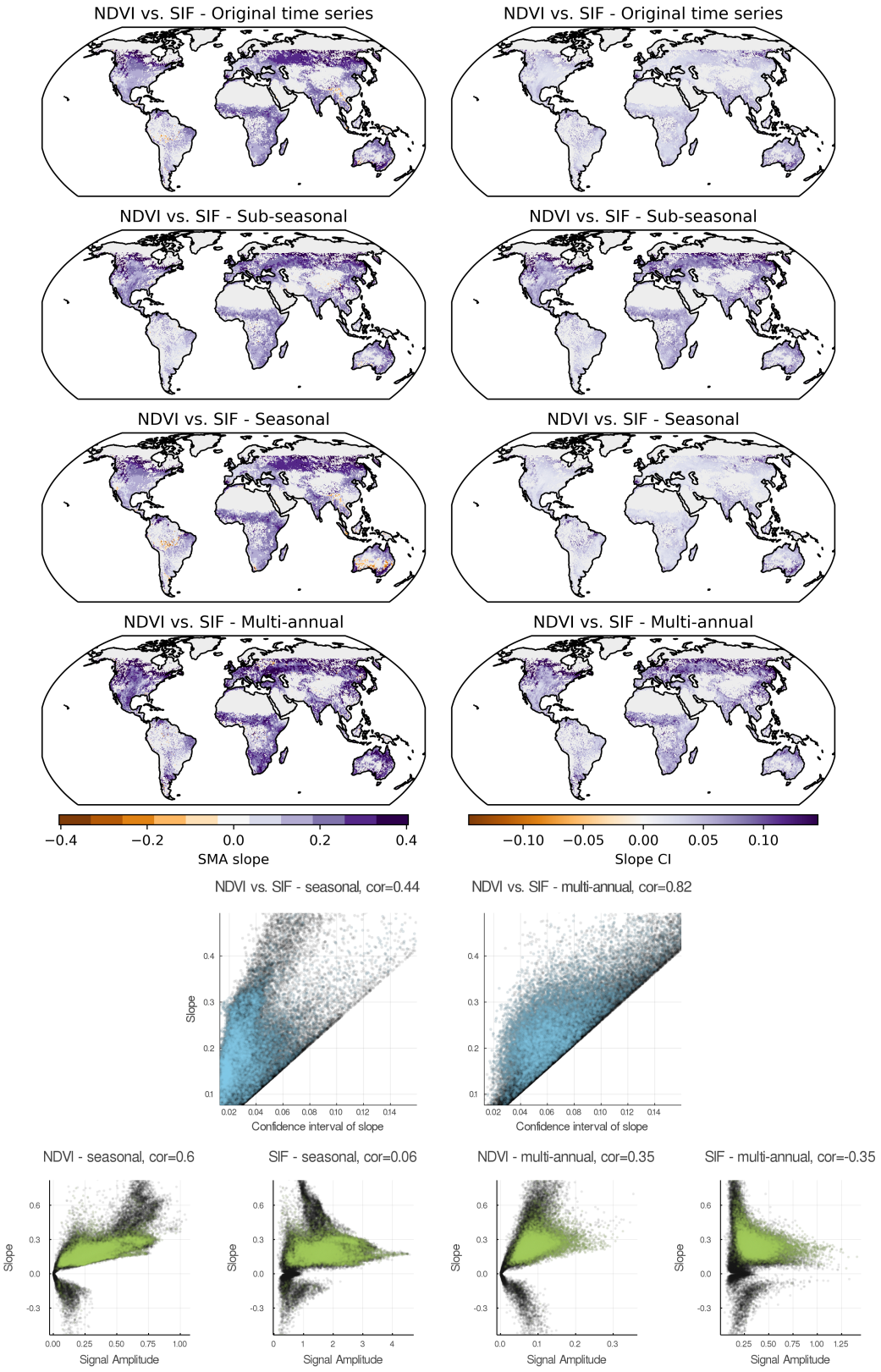

Figure S10: Time–scale specific slopes between NDVI vs. SIF. Top: Map of pixel–wise slopes (left) and confidence intervals of slopes (right). Middle: Slopes are plotted against their confidence intervals for seasonal (left) and multi–annual scales (right). Bottom: Scale–specific slopes are compared against matching scale–specific signal amplitudes separately for seasonal (left) and multi–annual time scale (right). Blue/Green points are retained in the analysis, grey points are filtered out. Correlations were calculated as Pearson correlation between non–filtered points.

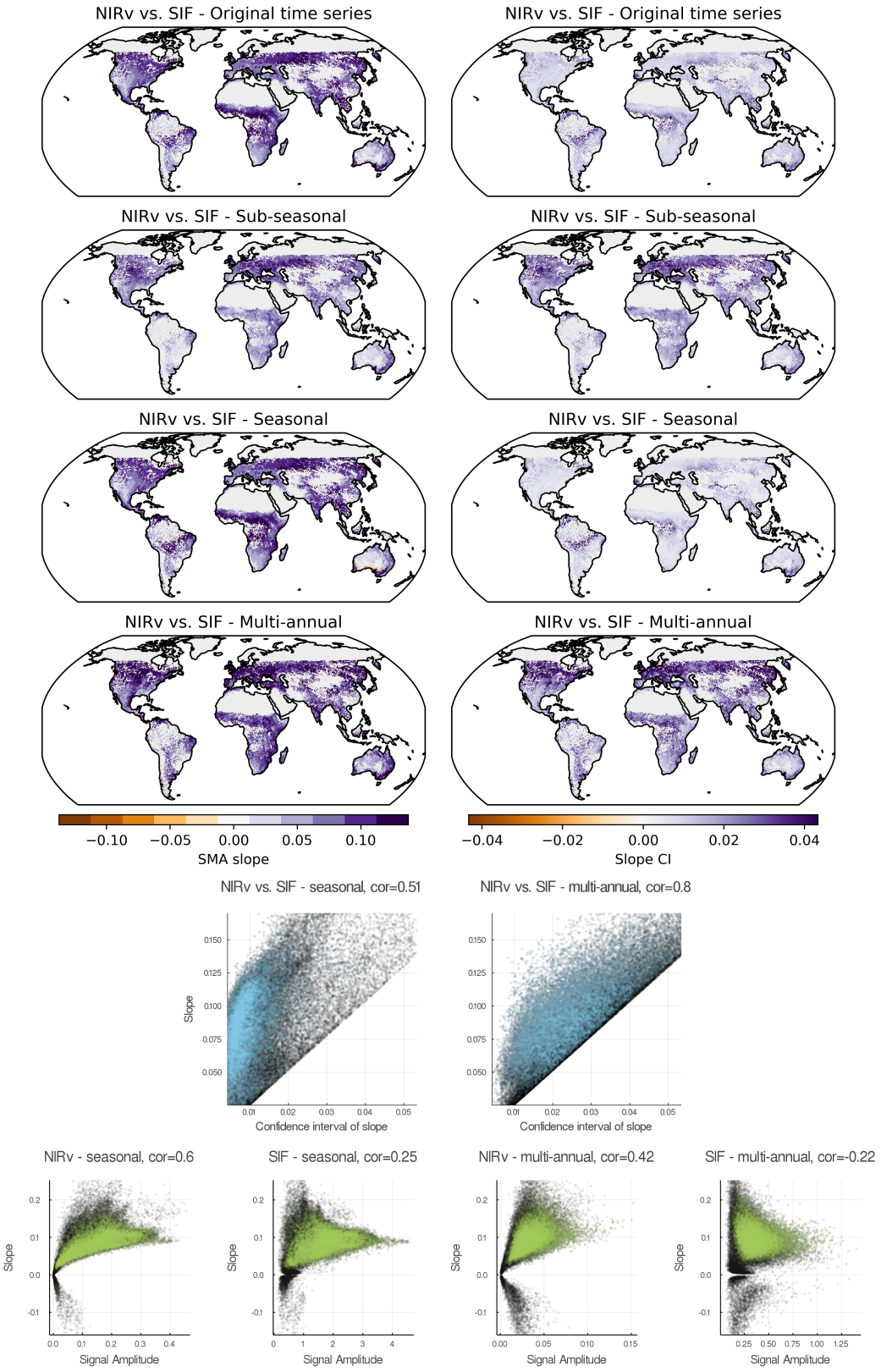

Figure S11: Time–scale specific slopes between NIRv vs. SIF. Top: Map of pixel–wise slopes (left) and confidence intervals of slopes (right). Middle: Slopes are plotted against their confidence intervals for seasonal (left) and multi–annual scales (right). Bottom: Scale–specific slopes are compared against matching scale–specific signal amplitudes separately for seasonal (left) and multi–annual time scale (right). Blue/Green points are retained in the analysis, grey points are filtered out. Correlations were calculated as Pearson correlation between non–filtered points.

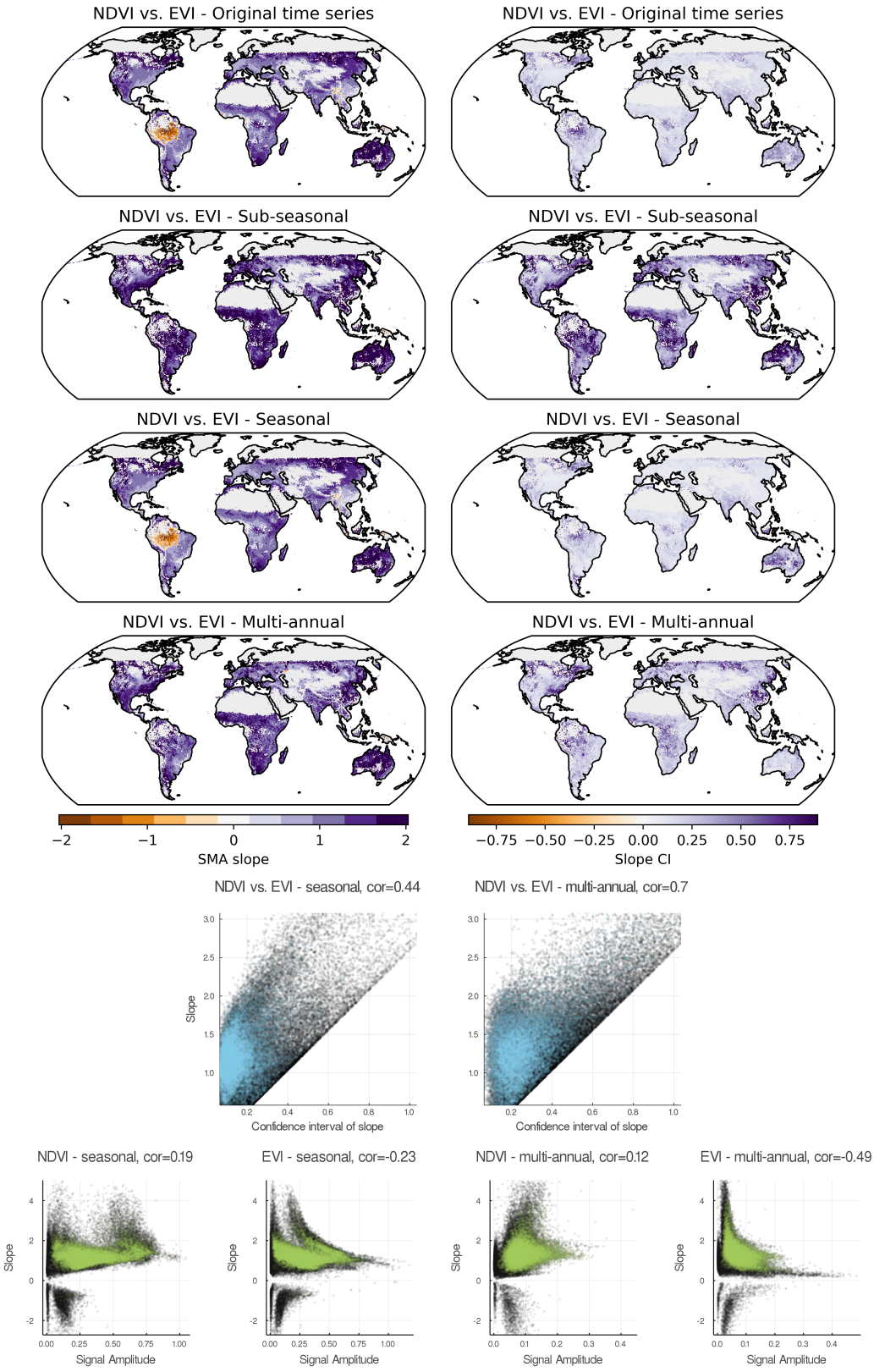

Figure S12: Time–scale specific slopes between NDVI vs. EVI. Top: Map of pixel–wise slopes (left) and confidence intervals of slopes (right). Middle: Slopes are plotted against their confidence intervals for seasonal (left) and multi–annual scales (right). Bottom: Scale–specific slopes are compared against matching scale–specific signal amplitudes separately for seasonal (left) and multi–annual time scale (right). Blue/Green points are retained in the analysis, grey points are filtered out. Correlations were calculated as Pearson correlation between non–filtered points.

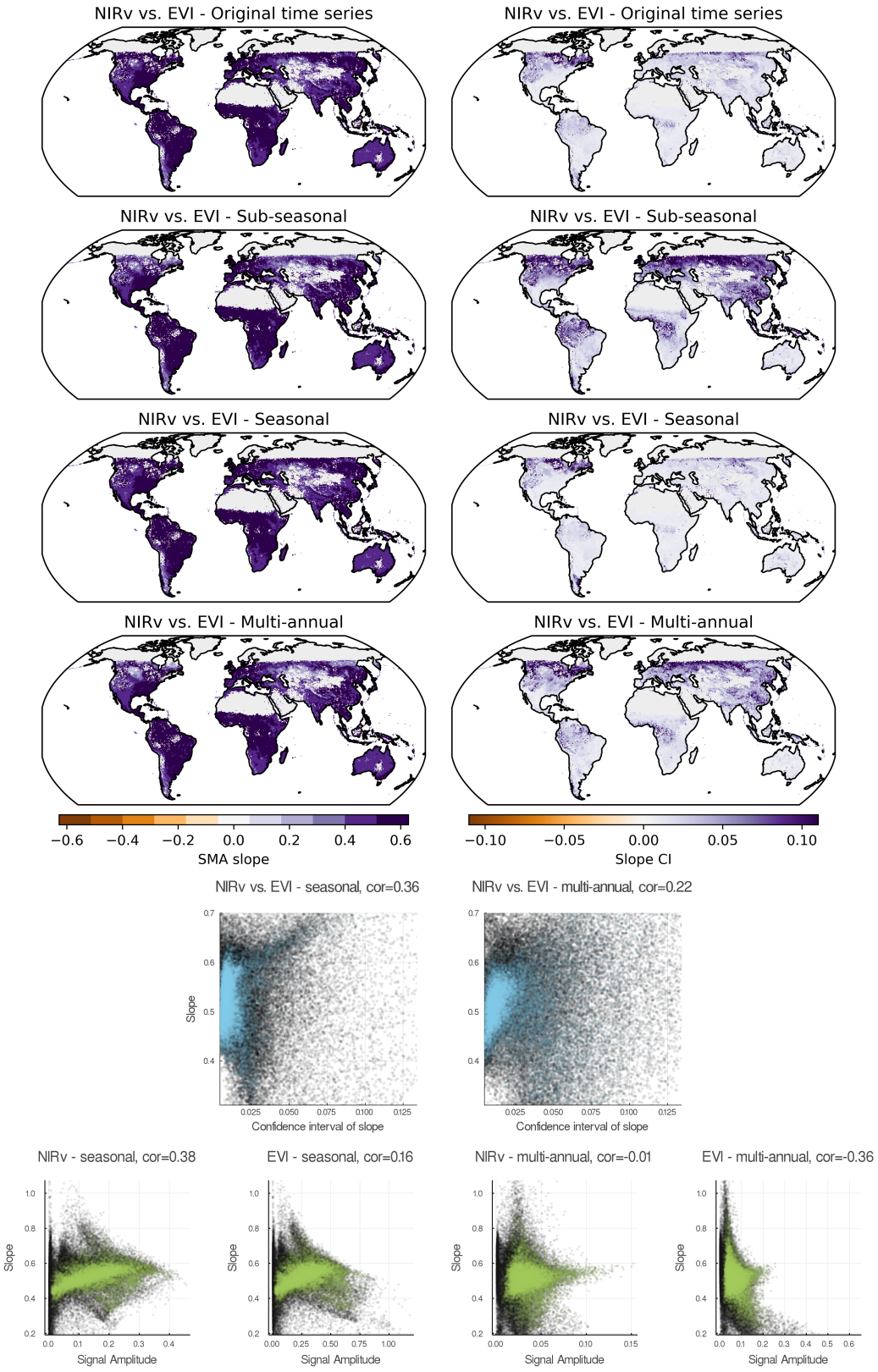

Figure S13: Time–scale specific slopes between NIRv vs. EVI. Top: Map of pixel–wise slopes (left) and confidence intervals of slopes (right). Middle: Slopes are plotted against their confidence intervals for seasonal (left) and multi–annual scales (right). Bottom: Scale–specific slopes are compared against matching scale–specific signal amplitudes separately for seasonal (left) and multi–annual time scale (right). Blue/Green points are retained in the analysis, grey points are filtered out. Correlations were calculated as Pearson correlation between non–filtered points.

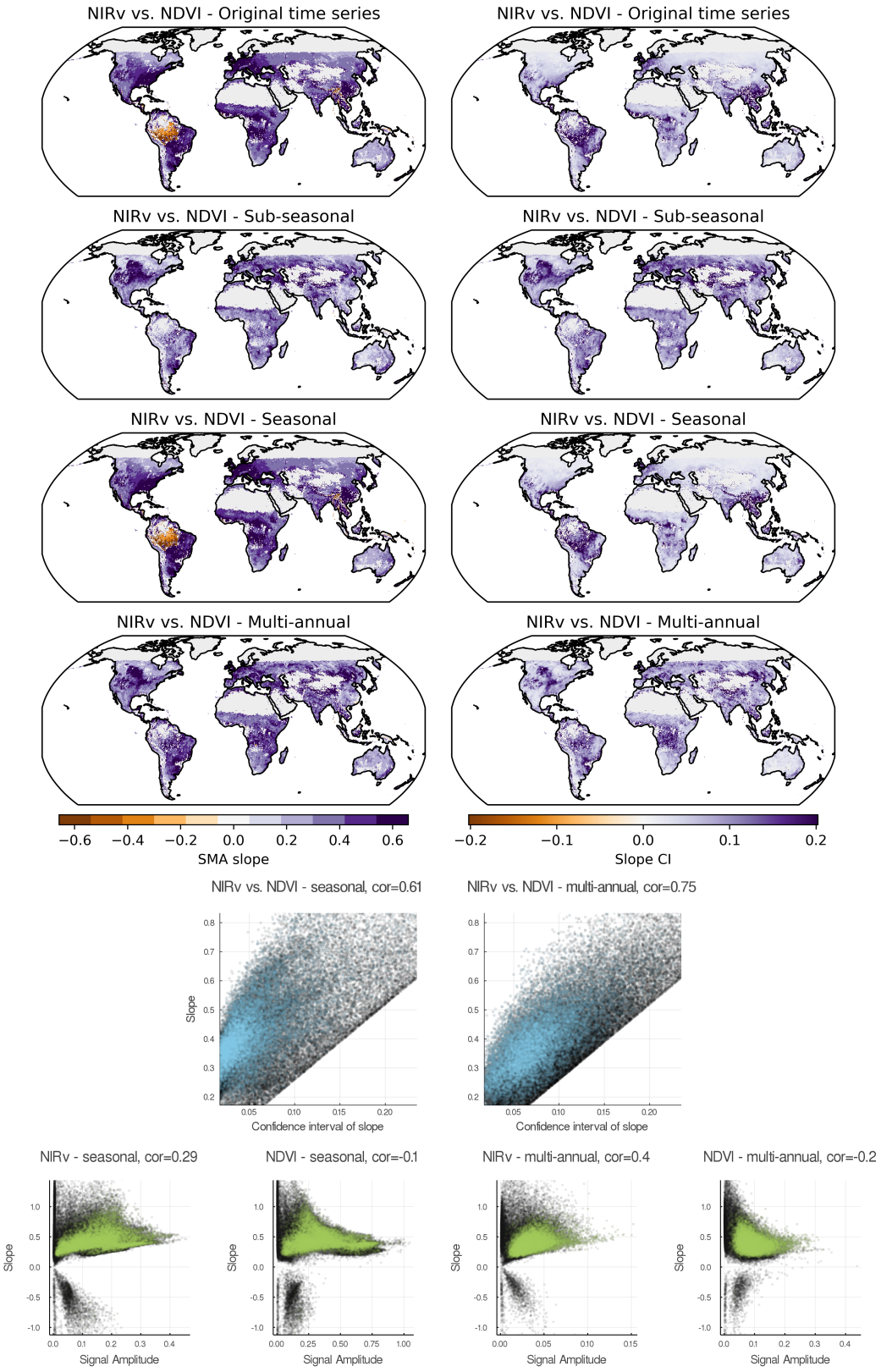

Figure S14: Time–scale specific slopes between NIRv vs. NDVI. Top: Map of pixel–wise slopes (left) and confidence intervals of slopes (right). Middle: Slopes are plotted against their confidence intervals for seasonal (left) and multi–annual scales (right). Bottom: Scale–specific slopes are compared against matching scale–specific signal amplitudes separately for seasonal (left) and multi–annual time scale (right). Blue/Green points are retained in the analysis, grey points are filtered out. Correlations were calculated as Pearson correlation between non–filtered points.

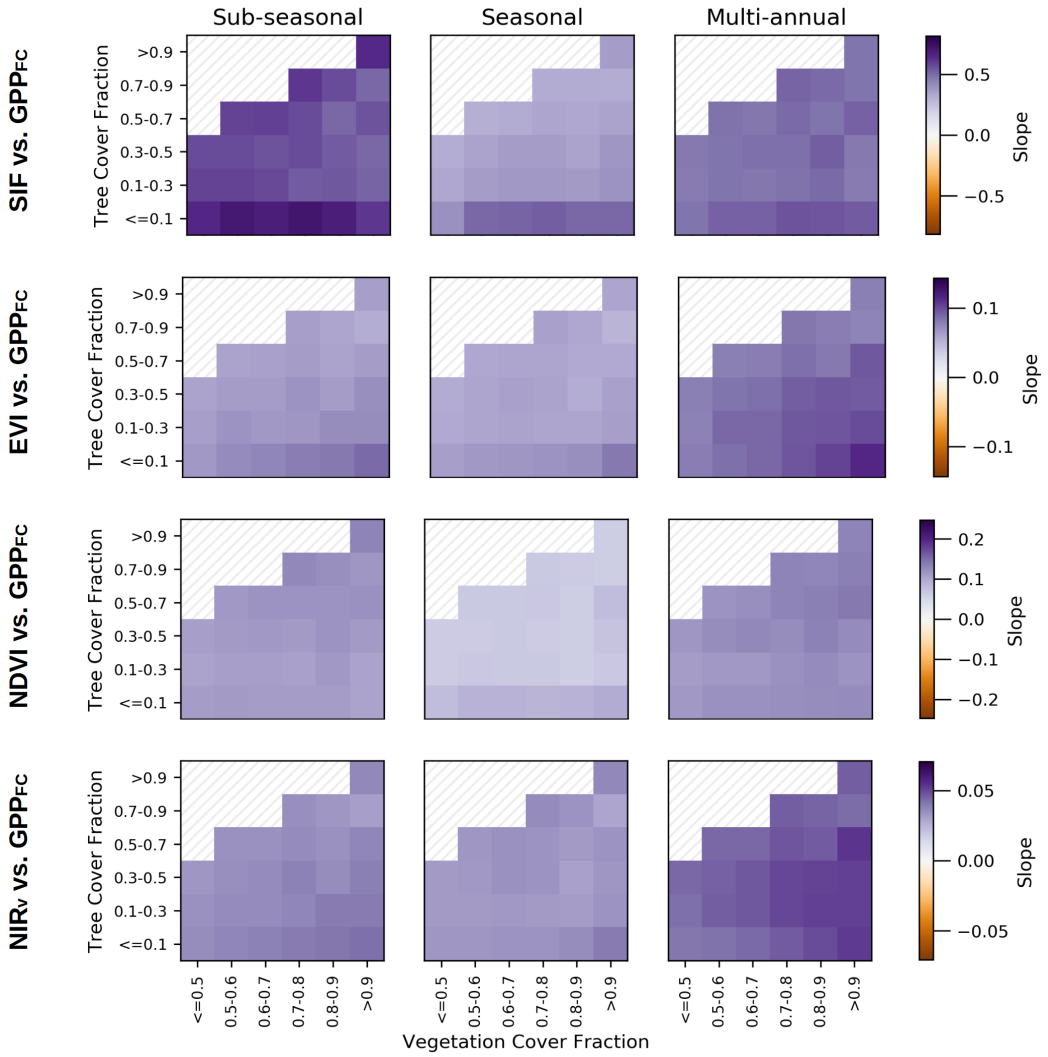

Figure S15: Time–scale specific slopes split by vegetation cover fraction and tree cover traction. Mean SMA slope of GPP_{FC} as x–variable with other vegetation proxies, split by climate and land cover class. Values represent mean slopes per class of pixels.

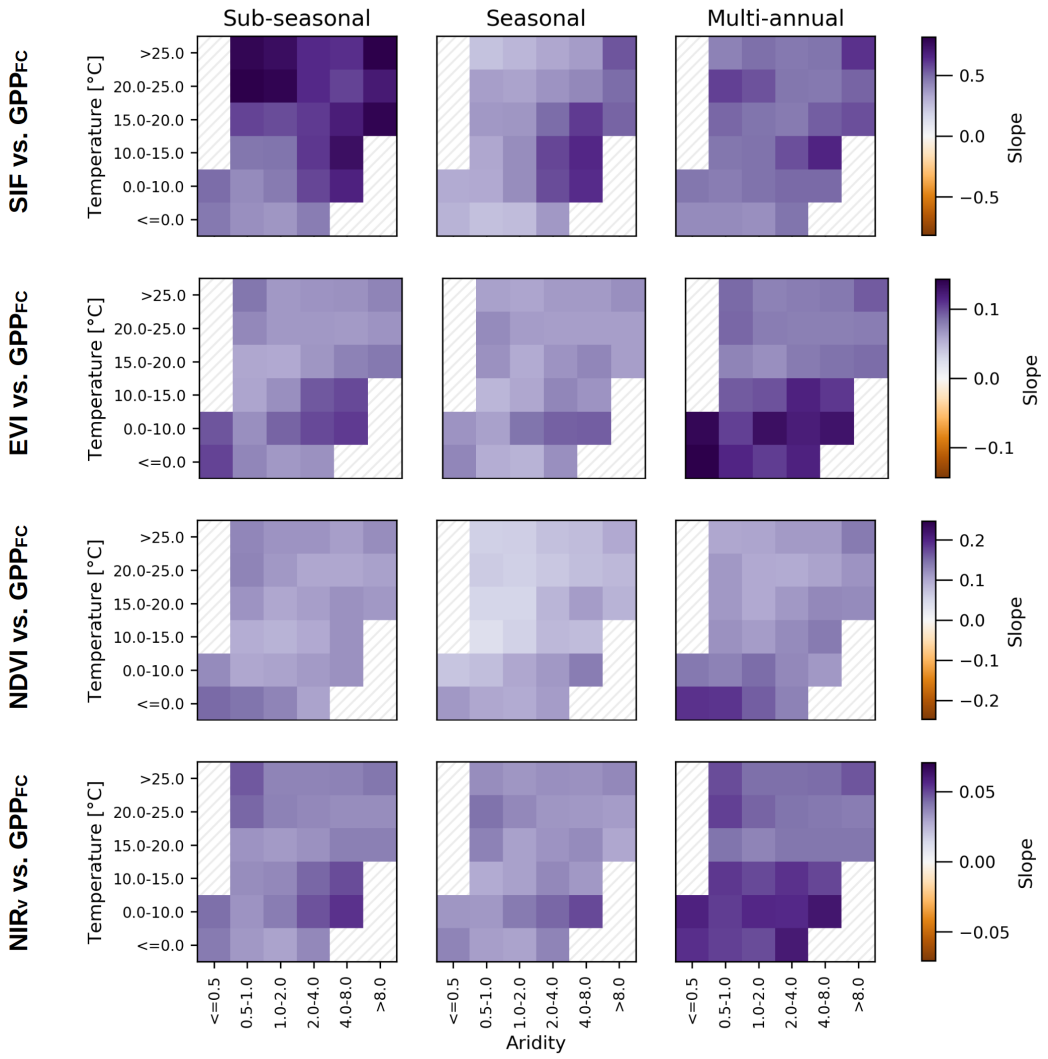

Figure S16: Time–scale specific slopes split by air temperature and aridity. Mean SMA slope of GPP_{FC} as x–variable with other vegetation proxies, split by climate and land cover class. Values represent mean slopes per class of pixels.

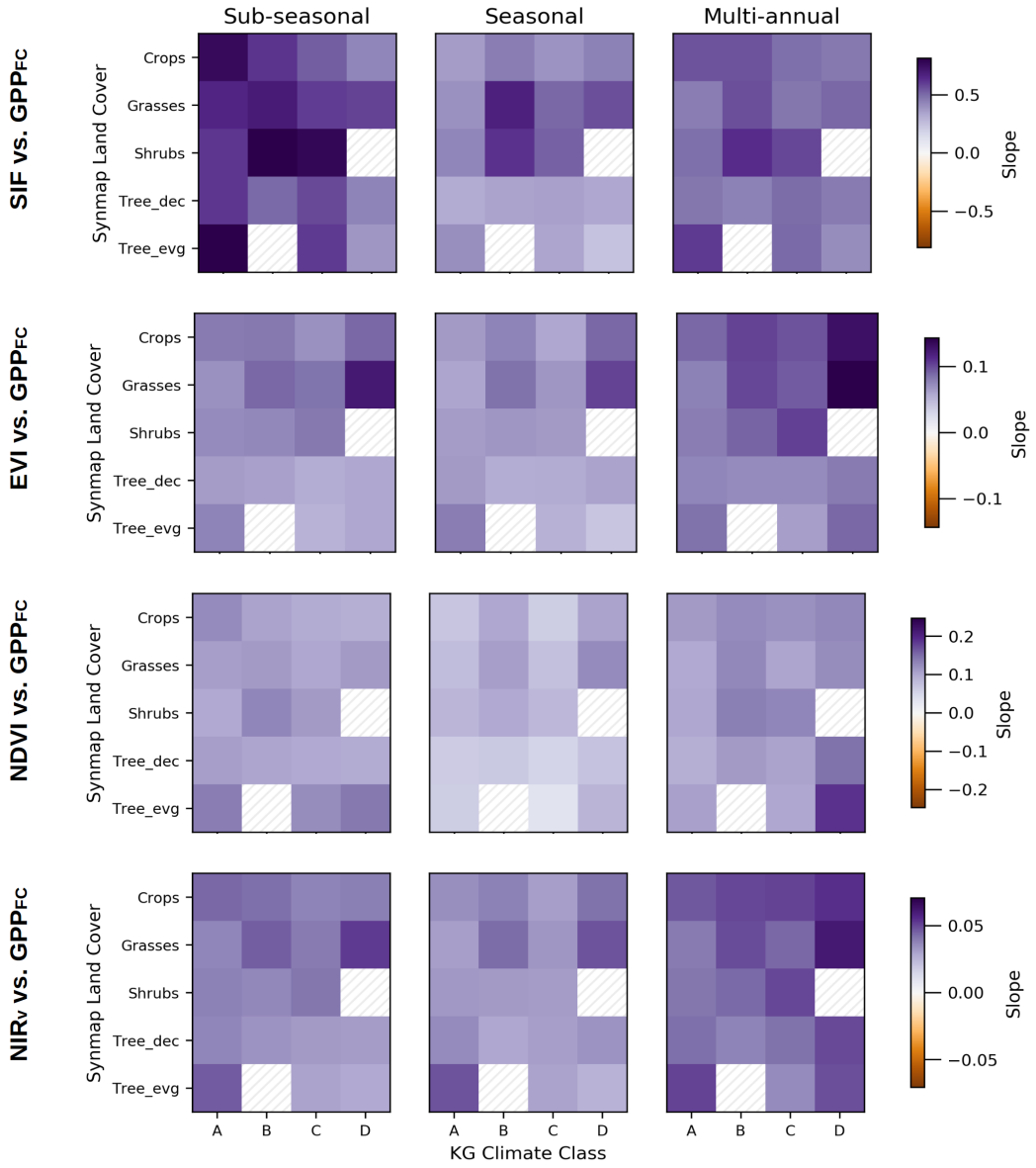

Figure S17: Time–scale specific slopes split by climate and vegetation type. Mean SMA slope of GPP_{FC} as x–variable with other vegetation proxies, split by climate and land cover class. Values represent mean slopes per class of pixels. KG: Koeppen–Geiger, A: equatorial, B: arid, C: warm temperate, D: snow, Tree_dec: Trees deciduous, Tree_evg: Trees evergreen.

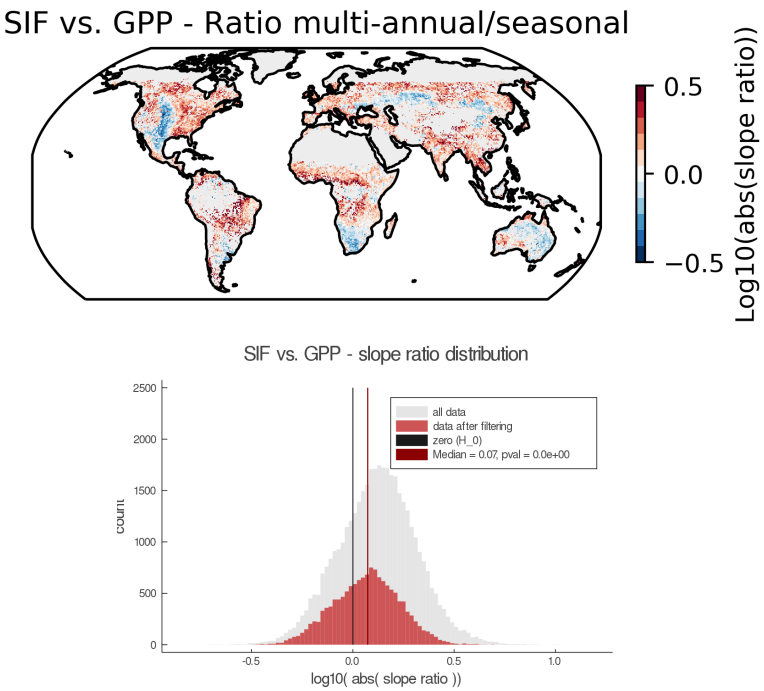

Figure S18: Maps and distributions of slope ratios for variable pair SIF vs. GPP. One–sample Wilcoxon signed rank tests were performed to test whether the median of the slope ratio distribution was not zero.

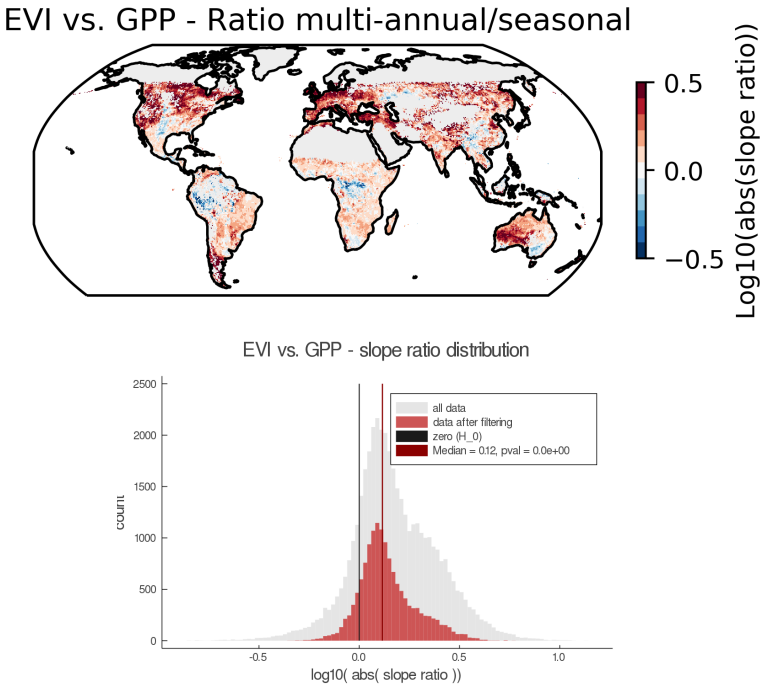

Figure S19: Maps and distributions of slope ratios for variable pair EVI vs. GPP. One–sample Wilcoxon signed rank tests were performed to test whether the median of the slope ratio distribution was not zero.

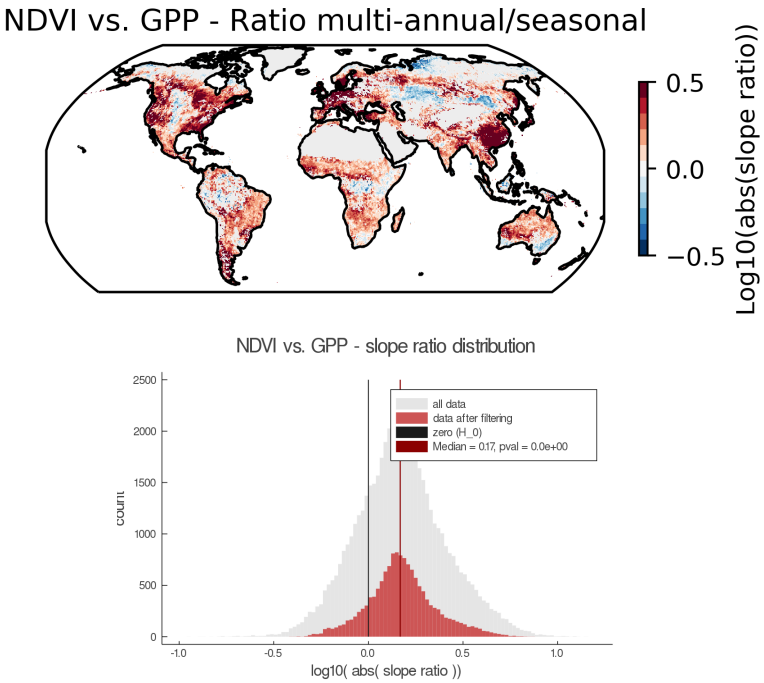

Figure S20: Maps and distributions of slope ratios for variable pair NDVI vs. GPP. One–sample Wilcoxon signed rank tests were performed to test whether the median of the slope ratio distribution was not zero.

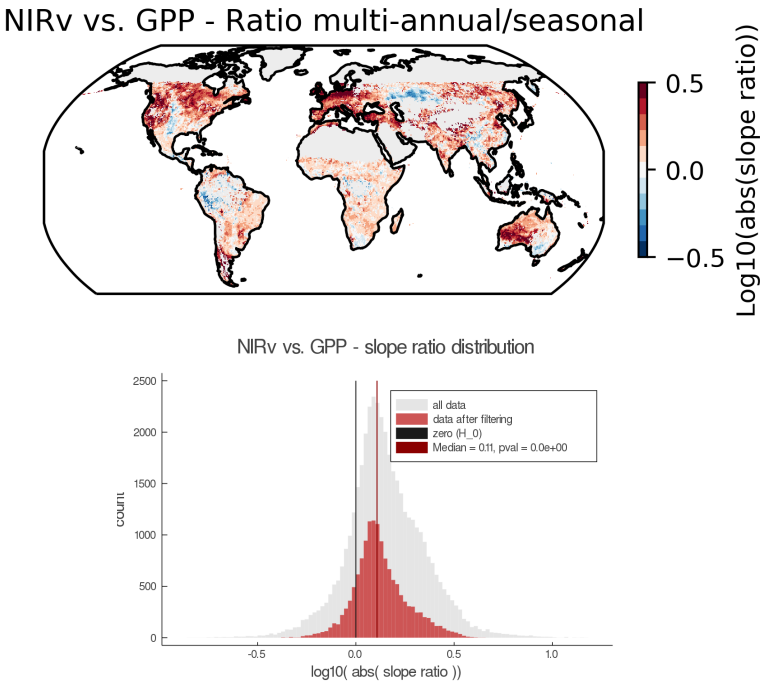

Figure S21: Maps and distributions of slope ratios for variable pair NIRv vs. GPP. One–sample Wilcoxon signed rank tests were performed to test whether the median of the slope ratio distribution was not zero.

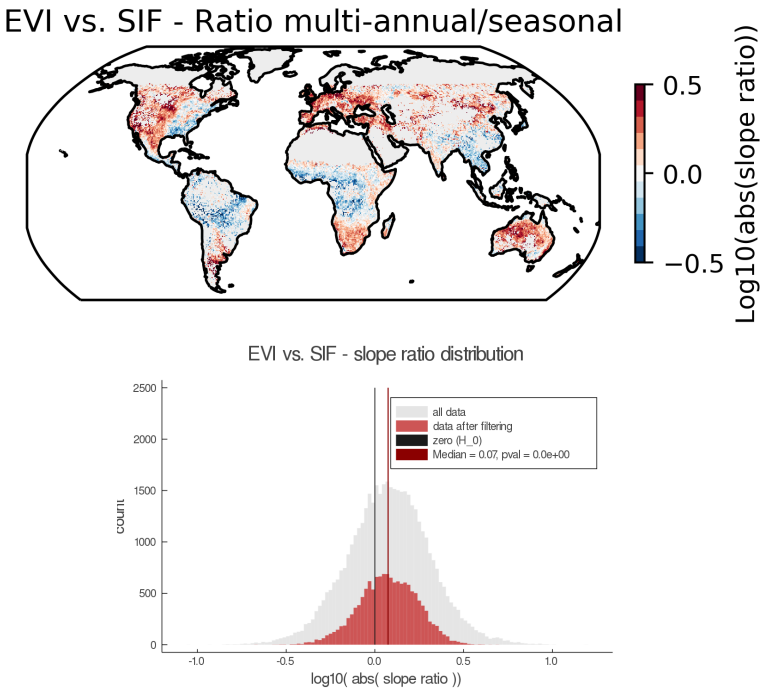

Figure S22: Maps and distributions of slope ratios for variable pair EVI vs. SIF. One–sample Wilcoxon signed rank tests were performed to test whether the median of the slope ratio distribution was not zero.

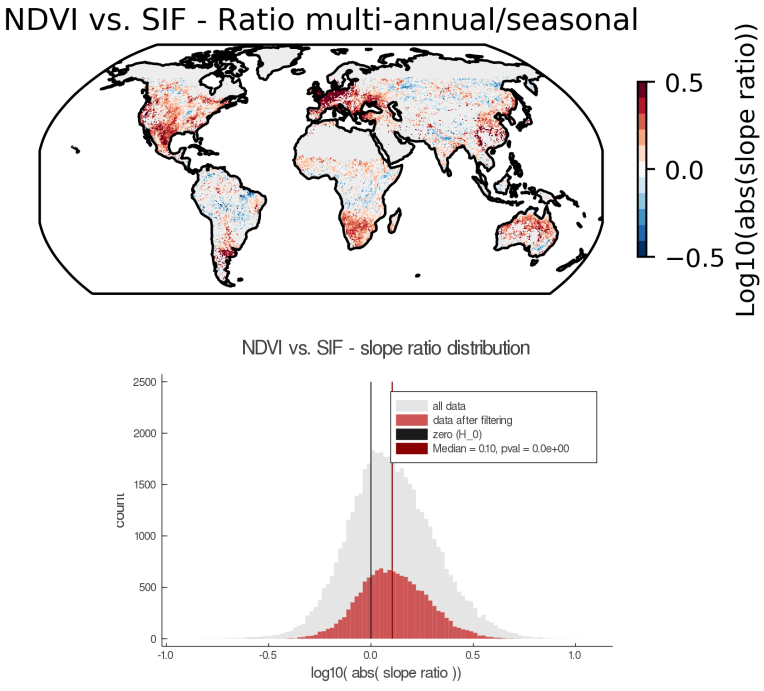

Figure S23: Maps and distributions of slope ratios for variable pair NDVI vs. SIF. One–sample Wilcoxon signed rank tests were performed to test whether the median of the slope ratio distribution was not zero.

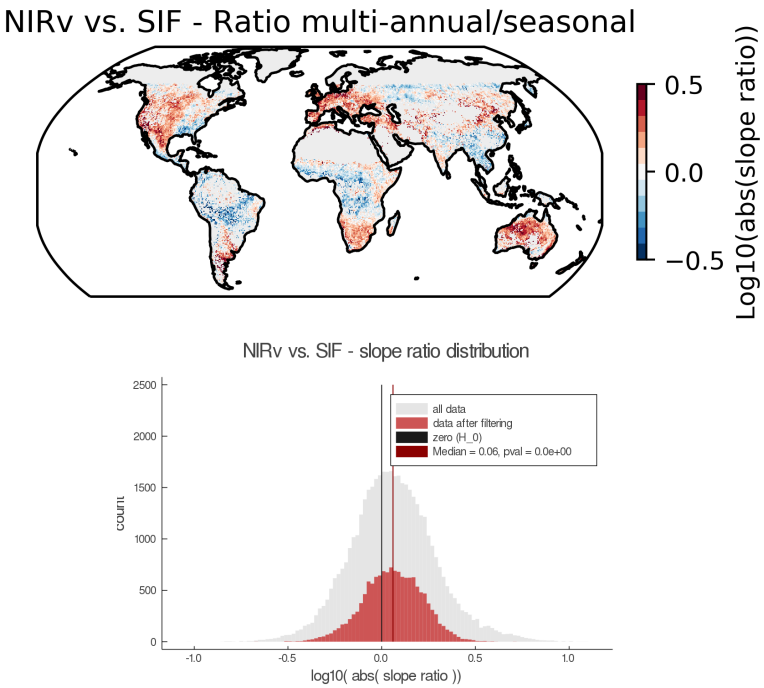

Figure S24: Maps and distributions of slope ratios for variable pair NIRv vs. SIF. One–sample Wilcoxon signed rank tests were performed to test whether the median of the slope ratio distribution was not zero.

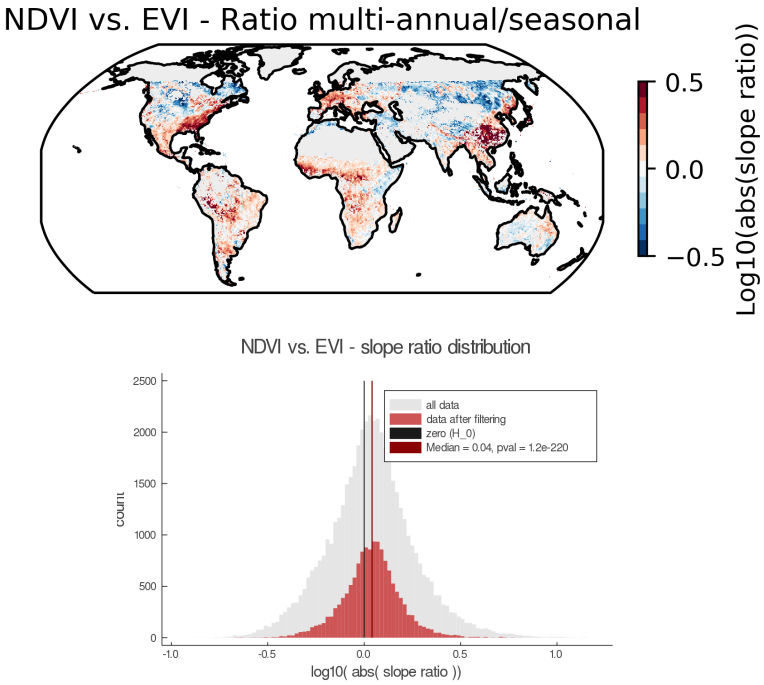

Figure S25: Maps and distributions of slope ratios for variable pair NDVI vs. EVI. One–sample Wilcoxon signed rank tests were performed to test whether the median of the slope ratio distribution was not zero.

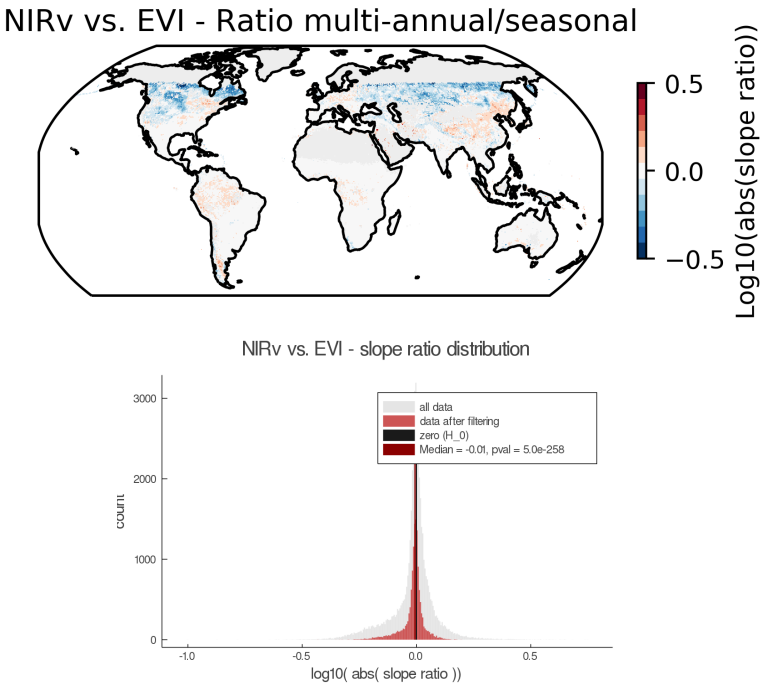

Figure S26: Maps and distributions of slope ratios for variable pair NIRv vs. EVI. One–sample Wilcoxon signed rank tests were performed to test whether the median of the slope ratio distribution was not zero.

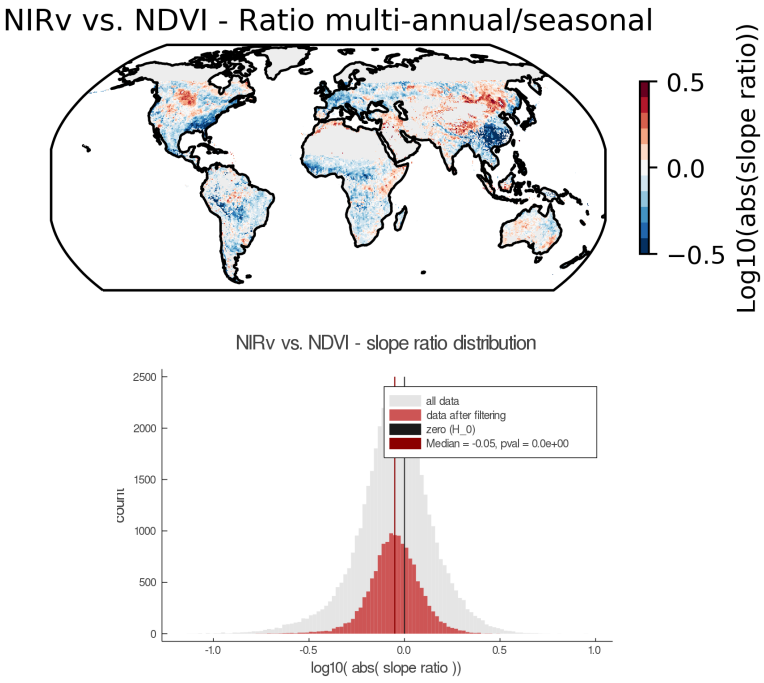

Figure S27: Maps and distributions of slope ratios for variable pair NIRv vs. NDVI. One–sample Wilcoxon signed rank tests were performed to test whether the median of the slope ratio distribution was not zero.

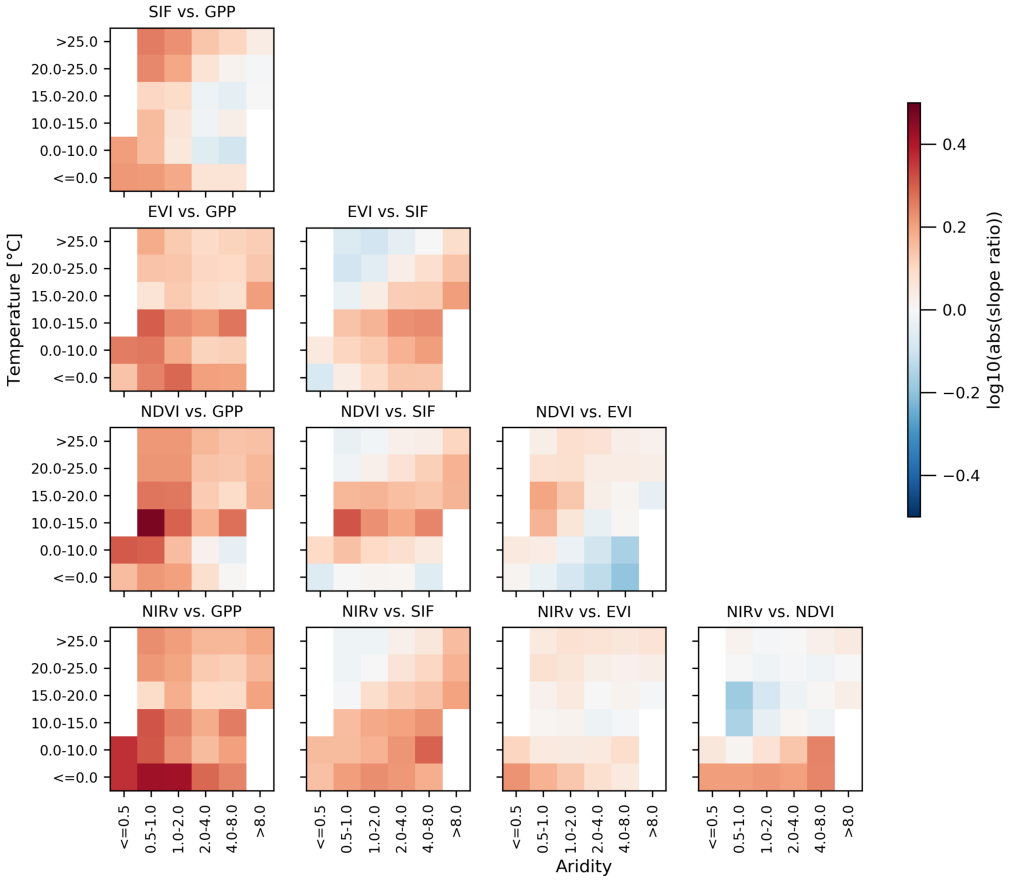

Figure S28: Pairwise slope ratios for all combinations of variables split by mean air temperature and aridity. The naming convention follows "y–variable vs. x–variable".

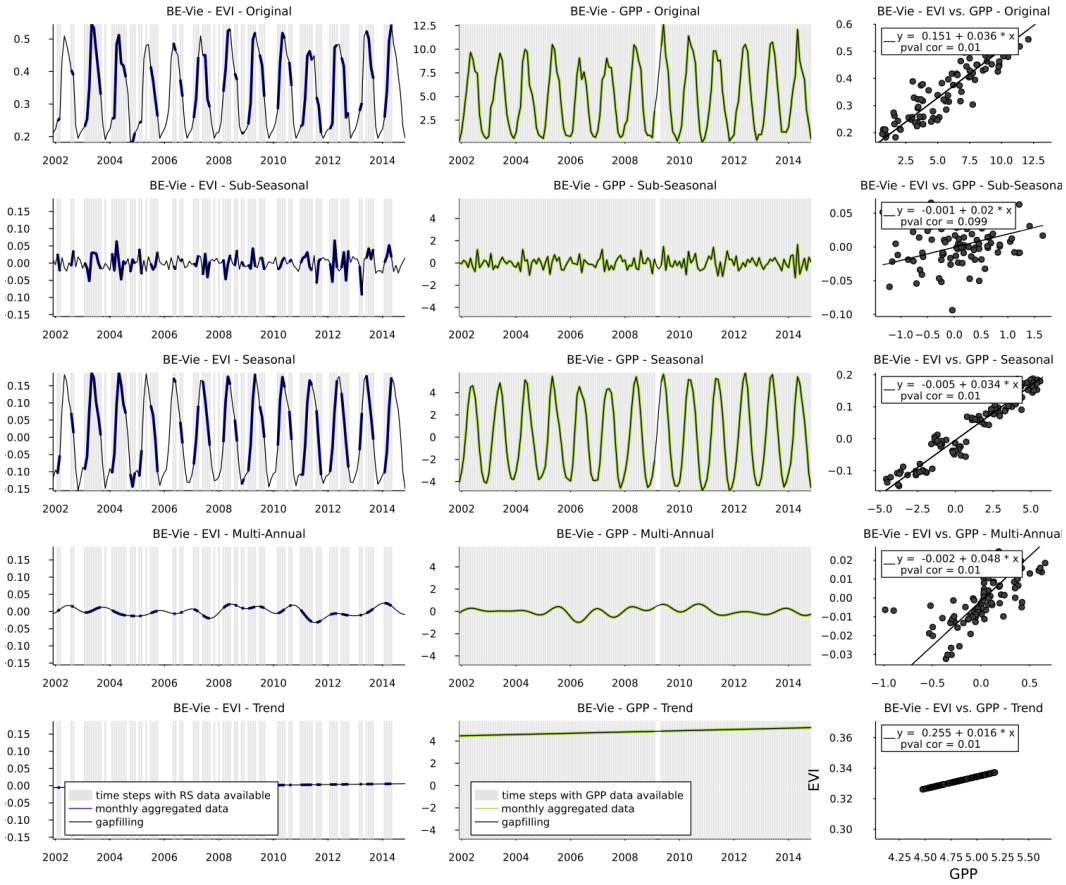

Figure S29: Example of Fluxnet and MODIS data aggregation and gapfilling for EVI (left) and GPP (middle) at Fluxnet site BE–Vie, and their time scale–specific slopes (right).

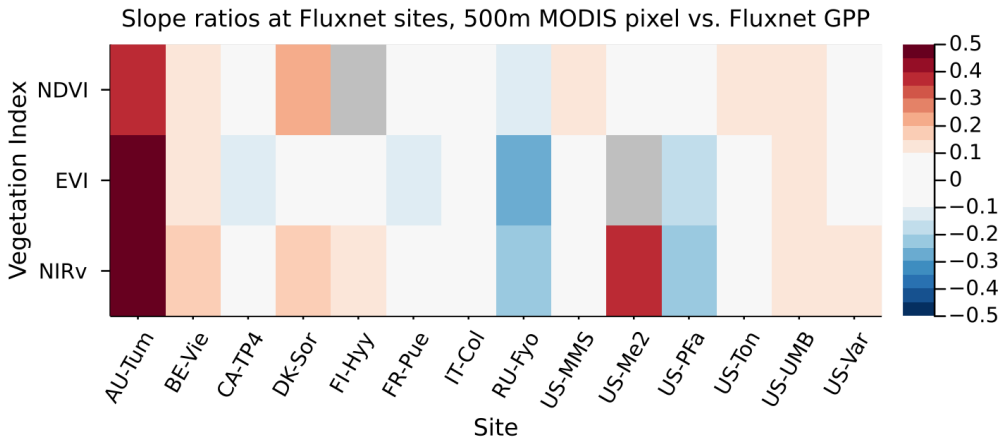

Variable	PFT	n	Sites	p-value	p-value abs ratios
NIRv	ENF	3	CA-TP4, FI-Hyy, RU-Fyo	0.01	0.01
NIRv	DBF	4	DK-Sor, IT-Col, US-MMS, US-UMB	0.43	0.09
EVI	DBF	3	DK-Sor, IT-Col, US-UMB	0.07	0.07
NDVI	DBF	4	DK-Sor, IT-Col, US-MMS, US-UMB	0.47	0.05

Figure S30: Comparative analysis of slope ratios at Fluxnet sites employing in–situ tower GPP estimates and vegetation proxies derived from 500m MODIS pixels at the 14 Fluxnet sites passing filtering criteria. Top: Site–level slope ratios between different MODIS vegetation proxies and and Fluxnet GPP. Bottom: Significance testing for slope ratios (top panel) per vegetation index and plant functional type. . For all PFTs where ¿2 sites passed quality control, the distribution of slope ratios for a given PFT x VI combination was tested against the hypothesis of being significantly different from zero by One-Sample T-Test (Table R1). Only slope ratios between NIRv and GPP in ENF were significantly different from zero (p¡0.05) in One-Sample-test. When considering the absolute magnitude of slope ratios (abs(log10(abs($slope_{ma}/slope_{seas}$)))), i. e. testing for a difference between seasonal and multi-annual slope without considering which slope was higher/lower, results for NDVI in DBF were also significant. It should be stressed that the sample size was very small (3–4 sites) and the slope ratios are here considered in log-space, i. e. any difference is deflated in comparison to a test in linear space. Hence the result could become clearer with more sites included. The color scale shows abs(log10($slope_{ma}/slope_{seas}$)), with red colors indicating higher multi–annual (absolute) slopes, and blue colors denoting higher (absolute) seasonal slopes. Grey color denotes that the given data point did not pass the significance filter. The differences in-between sites of the same PFT should also be stressed, indicating that additional explanatory factors may be needed to understand where multi-annual slopes differ from seasonal slopes. ENF: evergreen needleleaf forest, DBF: deciduous broadleaf forest.

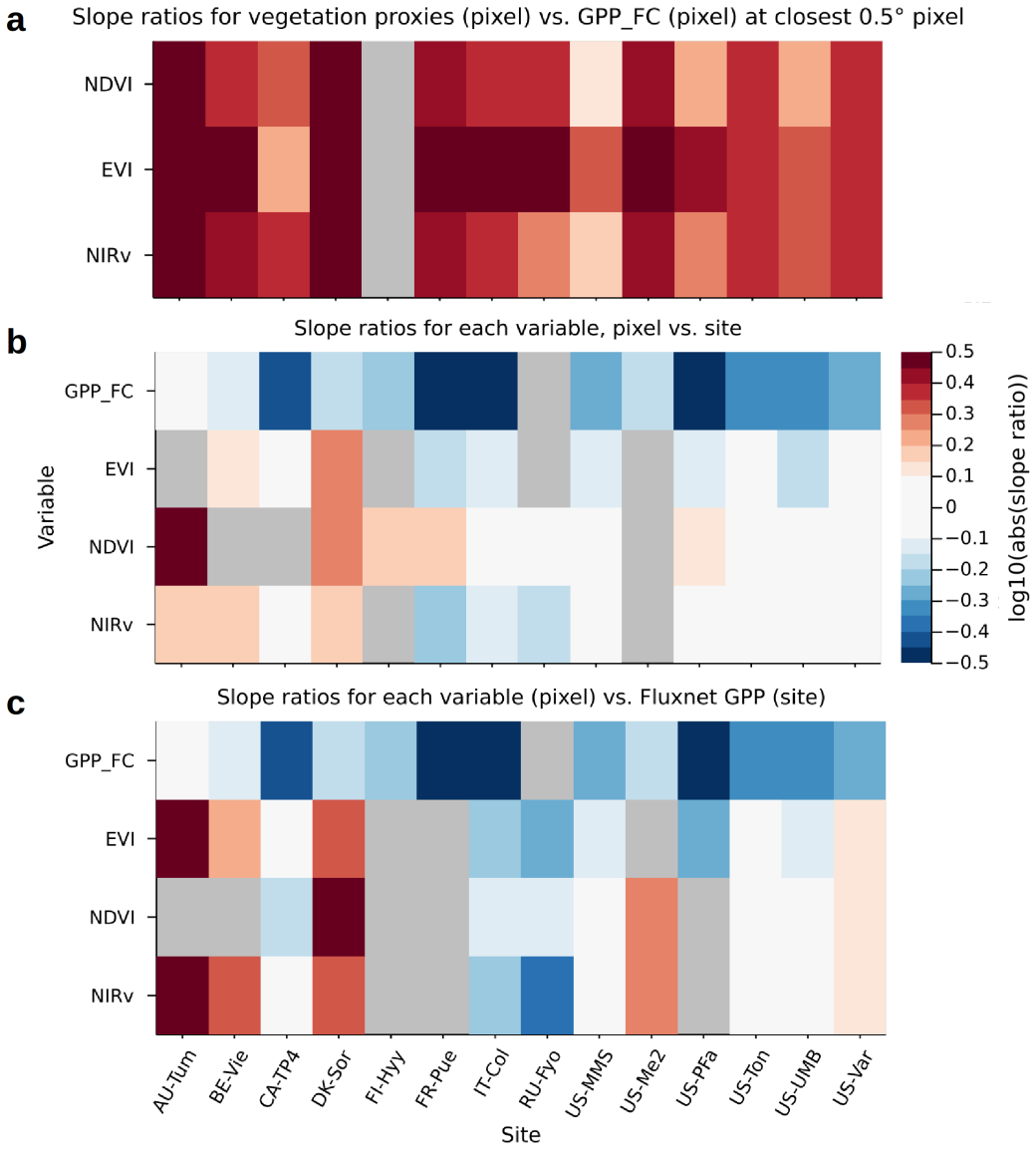

Figure S31: Comparison of site and pixel–scale data at the 14 Fluxnet sites passing filtering criteria. **a.** Pixel–scale slope ratios from global analysis (main Figs. 1-3) between vegetation indices and FLUXCOM GPP$_{FC}$ extracted at the closest pixel, **b.** Comparison of pixel vs. site data for each vegeation proxy. If similar ratios of multi–annual to seasonal variance is captured, slope ratios should be closer to zero, **c.** Comparison of pixel–scale vegetation proxies to site–scale Fluxnet GPP estimates.

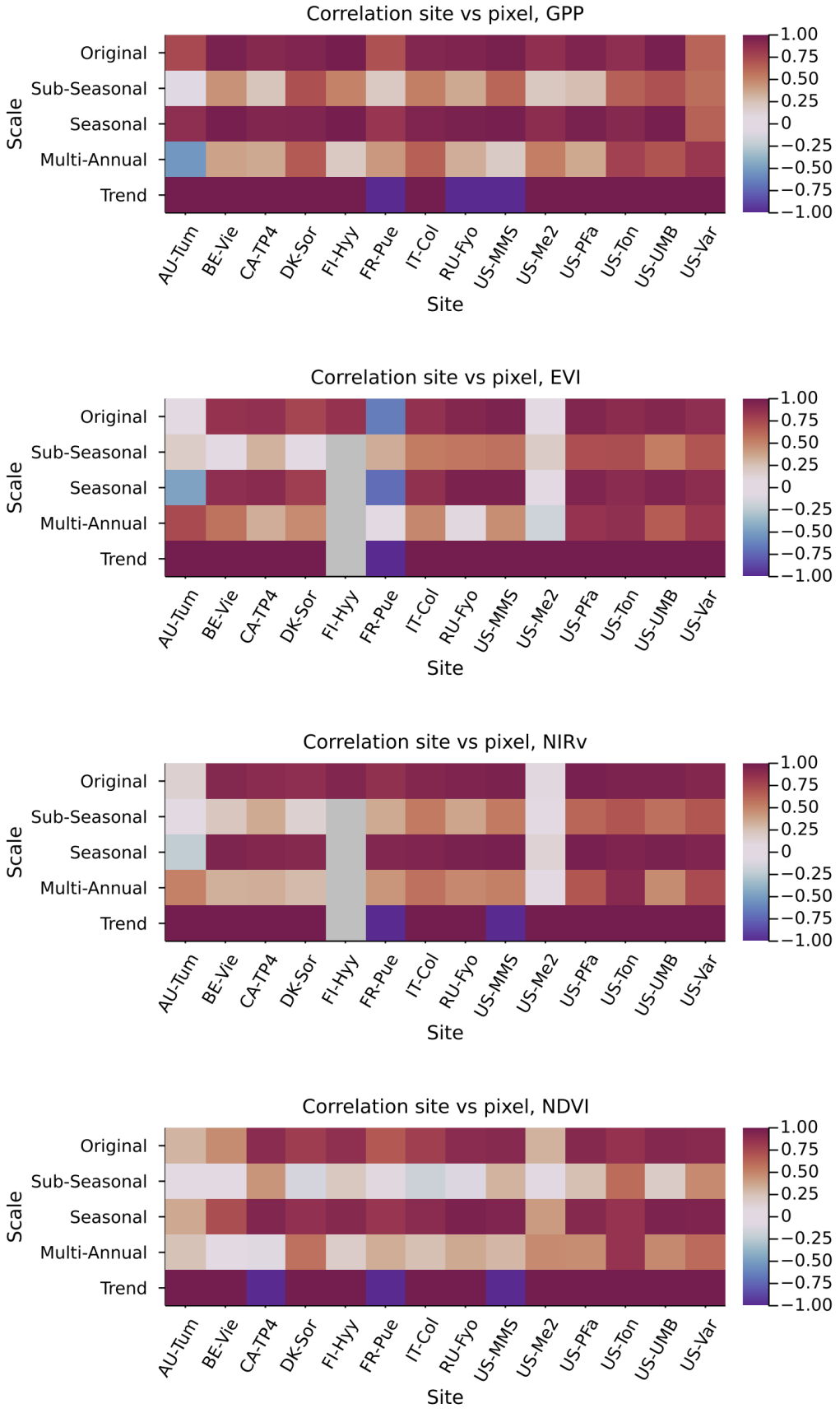

Figure S32: Correlations of site–scale and pixel–scale data at each time scale for vegetation indices at site versus pixel scale, and pixel-scale FLUXCOM GPP versus site–scale Fluxnet GPP at the 14 Fluxnet sites passing filtering criteria. Red colors denote positive, blue colors denote negative correlation.